Characterization and Regulation of Gap Junctions in Porcine Ciliary Epithelium

Stanley Ka-Lok Li,[1] Sze-Wan Shan,[1] Hoi-Lam Li,[1] Angela King-Wah Cheng,[1] Feng Pan,[1] Shea-Ping Yip,[2] Mortimer M. Civan,[3,4] Chi-Ho To,[1] and Chi-Wai Do[1]

[1]School of Optometry, The Hong Kong Polytechnic University, Hung Hom, Hong Kong, China
[2]Department of Health Technology and Informatics, The Hong Kong Polytechnic University, Hung Hom, Hong Kong, China
[3]Department of Physiology, Perelman School of Medicine, University of Pennsylvania, Philadelphia, Pennsylvania, United States
[4]Department of Medicine, Perelman School of Medicine, University of Pennsylvania, Philadelphia, Pennsylvania, United States

PURPOSE. Gap junctions provide a conduit between the intracellular fluids of the pigmented (PE) and non-pigmented (NPE) ciliary epithelial cells, and are therefore critical in the secretion of the aqueous humor (AH). However, opinions differ concerning the connexin (Cx) composition of the gap junctions. Therefore, we aimed to characterize the expression of Cx in the porcine ciliary epithelium (CE), a favorable model for humans; and determine the contribution of the highest expressed Cx to AH secretion.

METHODS. Freshly-harvested porcine CE cells were used. The mRNA and protein expressions of gap junctions were assessed by reverse transcription polymerase chain reaction (RT-PCR) and Western blotting (WB), respectively. The relative gene expressions of various Cx were determined by quantitative PCR. The gap junction permeability of isolated PE-NPE cell couplets was evaluated by Lucifer Yellow dye transfer.

RESULTS. Using RT-PCR and WB, Cx43, Cx45, Cx47, Cx50, and Cx60 were present in porcine CE, with Cx43 being the most abundant isoform, having over 200-fold higher expression than other Cx. Cx43 was primarily localized in the PE-NPE interface and the basolateral membranes of PE cells. Knockdown of Cx43 by siRNA significantly reduced gene and protein expressions, resulting in reduction of transcellular fluid flow by 90%.

CONCLUSIONS. Cx43 was found to be the major component of gap junctions in porcine CE. Consistent with results from a bovine model, our results support the important role of Cx43 in mediating AH secretion. This finding may shed light on the development of a novel ocular hypotensive agent.

Keywords: gap junctions, connexin 43, ciliary epithelium, aqueous humor formation, glaucoma

Glaucoma has been a leading cause of blindness worldwide, causing irreversible loss of sight. In principle, glaucoma could be treated by interrupting the pathogenesis of the disease or by neuroprotection of the retinal ganglion cells. Nevertheless, currently, lowering the intraocular pressure (IOP) remains the only effective clinical intervention to slow the onset and progression of glaucomatous vision loss. IOP can be lowered by reducing the rate of aqueous humor (AH) inflow, by increasing the outflow facility through the trabecular outflow pathway, or by shunting outflow through the pressure-insensitive uveoscleral outflow route.

AH inflow is secreted by the transfer of fluid and solutes across the dual-layered ciliary epithelium (CE). The solutes and fluid taken from the extracellular fluid by the pigmented ciliary epithelium (PE) are transferred to the nonpigmented ciliary epithelium (NPE). This fluid transfer is facilitated by intercellular gap junctions, thereby forming a functional syncytium to drive AH formation.[1,2] Heptanol, a nonspecific gap junction blocker, has been shown to inhibit the short-circuit current (Isc) and/or Cl⁻ secretion across the CE by 70% to 90% in rabbit,[3] ox,[4] and pig.[5] More importantly, heptanol has been demonstrated to elicit direct inhibition of transepithelial fluid transport across intact CE by ~80%.[6] The inhibitory effect is possibly mediated by the uncoupling of gap junctions (i.e., decrease in junctional currents and gap junction permeability) between PE and NPE cells.[7]

Generally, gap junction channels aggregate on the plasma membrane where they facilitate intercellular communication by exchanging solutes, metabolites, and signaling messengers between adjacent cells.[8] At present, over 20 gap junction connexin (Cx) isoforms have been identified.[9,10] Cx have been demonstrated to be widely expressed in different tissues and are tissue-specific.[10] The presence of gap junctions in the CE of rhesus monkeys and rabbits was first reported by Raviola and Raviola.[11,12] Later, biochemical and structural studies have determined the expression of various Cx in different species (Table).[13–18] Despite the distribution of various Cx isoforms identified in the CE of different species, the relative abundance of these Cx and their functional significance related to AH formation has not been clearly established.

The porcine eye has been considered a good model for studying AH inflow because of its similarities to the human eye, including its physical dimensions, anatomical characteristics, and electrolyte composition of the AH, as well as biocompat-

TABLE. Connexins (Cx) in the Ciliary Epithelium of Various Animal Species

Animal, Refs.	Location of Cx
Ox[13]	Cx43: PE-PE and PE-NPE interfaces
Rabbit[14]	Cx43: PE-PE and PE-NPE interfaces
	Cx50: NPE-NPE and PE-NPE interfaces
Rat[14,15]	Cx26: NPE (basolateral) and NPE-NPE interface
	Cx31: NPE (basolateral)
	Cx40: PE-NPE interface
	Cx43: PE-NPE interface
Mouse[16,17]	Cx43: PE-NPE interface
Pig[18]	Cx43: PE-NPE interface and PE (basolateral)
	Cx50: NPE (basolateral)

ibility with human eyes.[5,6,19–21] Recently, we have demonstrated that the stimulation of Isc by cAMP and forskolin in porcine CE[22] are in good agreement with results obtained in human tissue.[23] In this study, we aimed to characterize the expression of Cx isoforms in porcine CE, determine the relative abundance of various Cx, and investigate the functional significance of the most abundant Cx in mediating fluid movement from PE to NPE cells.

METHODS

Tissue Isolation

Freshly enucleated porcine eyes were obtained from a local slaughterhouse and transported to the laboratory on ice within 1 hour. Upon arrival, the porcine CE was immediately excised and rinsed with PBS (Affymetrix, Cleveland, OH, USA) thoroughly before use.

Reverse Transcription-Polymerase Chain Reaction (RT-PCR)

The total RNA of the isolated porcine CE was extracted with TaKaRa MiniBEST Universal RNA Extraction Kit (TaKaRa, Otsu, Shiga, Japan) according to the manufacturer's instructions. Reverse transcription of 1.0 μg/μL mRNA to cDNA was performed using a high capacity cDNA reverse transcription kit (Applied Biosystems, Foster City, CA, USA), followed by PCR using a master mix kit (HotStarTaq Plus; Qiagen, Germantown, MD, USA) with primers specific for different Cx isoforms (see Supplementary Table S1). The PCR products were separated in 1% to 2% agarose gels incorporated with a staining agent (Gel Red; Biotium, Hayward, CA, USA), and were visualized under UV light. Negative controls were performed for each pair of primers without cDNA template. The image was captured and analyzed using an imaging system (Azure C600; Azure Biosystems, Dublin, CA, USA). At least three biologic replicates were performed for each pair of primers.

Quantitative PCR (qPCR)

A two-step qPCR was performed using a PCR System (7500 Fast Real-Time; Applied Biosystems), followed by dissociation curve analysis using green master mix (Fast SYBR; Applied Biosystems). A total reaction volume of 10 μL containing 0.5 μL cDNA, 0.5 μM of each primer, and 5 μL 2X master mix was used. The primers used for qPCR are listed in Supplementary Table S2. The qPCR protocol comprised the following steps: 50°C for 2 minutes, 95°C for 10 minutes, 40 cycles of 95°C for

15 seconds, and 60°C for 1 minute, followed by a dissociation step from 60°C to 95°C for dissociation curve analysis. GAPDH was used as the reference gene. Each sample was run in triplicate, and the averaged results were used to determine the relative expression of Cx by the ΔΔCt method.[24]

Immunoblotting

The isolated pieces of porcine CE were homogenized by sonication in radioimmunoprecipitation assay (RIPA) buffer (Abcam, Cambridge, MA, USA) with protease inhibitor (cOmplete ULTRA Tablets, Mini, EASYpack; Roche, Mannheim, Germany), and cleared by centrifugation. Each sample of 20 to 100 μg protein was subjected to electrophoresis (SDS-PAGE), and electroblotted onto poly-vinylidene difluoride (PVDF) membranes (BioRad Laboratories, Hercules, CA, USA). After blocking with 5% nonfat dry milk, the membranes were incubated with primary antibody against specific Cx isoform at 4°C overnight. The membranes were incubated with appropriate horseradish peroxidase-conjugated secondary antibodies for 1 hour. The protein bands were visualized using a chemiluminescent substrate (SuperSignal West Pico Chemiluminescent Substrate; Thermo Fisher Scientific, Waltham, MA, USA) and were captured using an imaging system (Azure Biosystems). The relative intensity of the bands was determined using software Image-J (http://imagej.nih.gov/ij/; provided in the public domain by the National Institutes of Health, Bethesda, MD, USA), and normalized to the band intensity of GAPDH. At least three biologic replicates were performed for each Cx. The primary and secondary antibodies used are listed in Supplementary Table S3.

Hematoxylin and Eosin (H&E) Staining and Immunohistochemistry

The ocular preparations were fixed in 4% paraformaldehyde, embedded in paraffin and sectioned. The sections were deparaffinized, and rehydrated with PBS. For H&E staining, the sections were stained with hematoxylin for 3 minutes and then rinsed with running water. Following differentiation with acid ethanol (1% HCl in 70% alcohol) for 5 minutes, the sections were rinsed with running water, stained with eosin Y for 5 minutes, and dehydrated in increasing concentration of alcohol, and cleared in xylene. The slides were then mounted and imaged via an inverted fluorescence microscope (Eclipse 18 Ti-Sl; Nikon Corp, Tokyo, Japan). For immunohistochemistry, after washing with PBS with 0.1% Triton X-100, the sections were blocked with 5% goat serum (Vector Laboratories, Burlingame, CA, USA), followed by incubation with primary antibody against Cx43 (Cell Signaling, Danvers, MA, USA) at 4°C overnight. The sections were then washed and incubated with FITC-conjugated secondary antibody (Invitrogen, Camarillo, CA, USA) and DAPI (Molecular Probes, Invitrogen) at room temperature for 1 hours. The slides were mounted with medium (VECTASHIELD Antifade Mounting Medium; Vector Laboratories), and imaged via a scanning laser confocal microscope (Zeiss LSM800; Jena, Germany).

siRNA Knockdown

Similar to our previous studies,[7,22] porcine CE cells were isolated from the freshly dissected porcine eyes by incubating with 0.25% trypsin (Gibco, Grand Island, NY, USA) for 30 minutes at 37°C. The isolated cells were incubated in high-glucose Dulbecco's modified Eagle's medium (Gibco) supplemented with 1% penicillin-streptomycin (Gibco) and 10% fetal

bovine serum (Gibco) in a humidified 5% CO_2 incubator at 37°C overnight. Thereafter, gene silencing was achieved using Cx43-siRNA and scrambled-siRNA. The siRNA sequences targeting Cx43 were forward 5′-CUGAUGACCUGGAGAU CUA(dTdT)-3′ and reverse 5′-UAGAUCUCCAGGUCAU CAG(dTdT)-3′; and the scrambled siRNA sequences were forward 5′-CCUACGCCACCAAUUUCGU(dTdT)-3′ and reverse 5′-ACGAAAUUGGUGGCGUAGG(dTdT)-3′ (Molecular Informatrix Laboratory, Hong Kong). The 5′ end of the forward strands were labeled with FAM to assist the identification of transfected cells. The transfection was achieved with 50 nM siRNAs using a transfection reagent (HiPerfect; Qiagen, Hamburg, Germany). After a 24-hour incubation, the cells were processed for qPCR and Western blot analysis.

Lucifer Yellow Dye Transfer

The procedures were similar to those described previously.[7] The bathing solution contained (in mM) 113.0 NaCl, 4.56 KCl, 21.0 $NaHCO_3$, 0.6 $MgSO_4$, 7.5 D-Glucose, 1.0 L-Glutathione reduced, 1.0 Na_2HPO_4, 10.0 HEPES, and 1.4 $CaCl_2$. The pH and osmolality of the bathing solution were adjusted to 7.4 and 300 mOsm/kg, respectively. The pipette solution comprised (in mM) 25 NaCl, 110 L-aspartic acid, 120 N-Methyl-D-glucamine (NMDG), 0.38 $CaCl_2$, 12 4-(2-hydroxyethyl)-1-piperazineethanesulfonic acid (HEPES) and 1 mg/mL Lucifer yellow CH, lithium salt (Invitrogen).

The PE cells of the isolated FAM-labeled PE-NPE couplets were chosen to be the donor cells. Similar to the whole-cell patch clamp experiment, a tight seal between the micropipette and the cell membrane was formed. After rupturing the plasma membrane, the Lucifer yellow (LY) dye in the micropipette solution diffused to the PE (donor) cell, and subsequently to the NPE (recipient) cell. Images were captured every 30 seconds for 30 minutes by an inverted fluorescence microscope (Nikon Corp). F ratio (fluorescence intensity in NPE to that of PE cell) was used for fluid flow analysis.

Statistics

All data were presented as mean ± SEM. Student's t-test or 1-way ANOVA was used for data analysis (GraphPad Prism 5; GraphPad Software, Inc., San Diego, CA, USA). A P value less than 0.05 was considered statistically significant.

RESULTS

Expression of Connexin (Cx) in Porcine CE

RT-PCR revealed the presence of the mRNAs of Cx37, Cx43, Cx45, Cx47, Cx50, and Cx60 in native porcine CE (Fig. 1). All the band sizes shown in the samples agreed with those expected, suggesting that the primers were specific for the target genes. In contrast, Cx26, Cx30.3, Cx31, Cx32, and Cx40 were not detected despite various pairs of primers being used. After the initial screening by RT-PCR, the protein expression of the identified Cx isoforms were determined by WB. The presence of Cx43, Cx45, Cx47, Cx50, and Cx60 proteins was confirmed and the band sizes were consistent with those shown in the positive control (Fig. 2). Different porcine tissues including heart, lung, and lens were used as positive controls for different Cx isoforms, respectively, due to their abundance and expression specificity in different tissues. Although Cx37 was identified at mRNA level by RT-PCR, it was not detected at protein level by WB.

Relative Expression and Distribution of Cx Isoforms

Quantitative RT-PCR (qPCR) was used to investigate the relative expression levels of the Cx isoforms in freshly harvested porcine CE cells. Our results showed that the gene expression of Cx43 was over 200-fold higher than those of all other expressed Cx isoforms observed (Fig. 3). The second most expressed Cx isoform was Cx45, but its expression level was only 0.4% of Cx43. The expression levels of other Cx were < 0.2% of that of Cx43.

Since Cx43 was the most abundant Cx found in porcine CE, its localization was studied by immunohistologic analysis. As shown in Figure 4, Cx43 was primarily localized at the apical surface linking PE and NPE cells, as well as on the basolateral membrane of PE cells. Our results support the hypothesis that Cx43 is the major Cx present in porcine CE and that it may be responsible for ion and fluid movement between PE and NPE cell layers.

Effect of Cx43 Knockdown on Dye Transfer

Based on the results of gene and protein expressions, together with the previous findings showing the crucial role of gap junctions between PE and NPE cells in regulating AH secretion,[6,7] we speculated whether Cx43 was important in transferring fluid from PE to NPE cells leading to AH formation in pigs. To test this hypothesis, we used small interfering RNA (siRNA) to knockdown the expression of Cx43 and determined whether it affected the fluid movement across isolated porcine PE-NPE cell couplets by using the LY dye transfer technique. After a 24-hour transfection with 50 nM siRNA against Cx43 or scrambled siRNA, the relative mRNA expressions of Cx43 in porcine CE cells was determined by qPCR. As shown in Figure 5A, the mRNA expression of Cx43 in porcine CE cells were decreased by 59% ± 3% with siRNA treatment against Cx43 compared to the cells treated with scrambled siRNA ($N = 4$, $P < 0.001$, Student's t-test). Similarly, the Cx43 protein expression in porcine CE was reduced by 71% ± 13% in preparations treated with siRNA against Cx43 compared to the control with scrambled siRNA (Fig. 5B, $N = 3$, $P < 0.01$, Student's t-test).

The changes in ratios of relative fluorescence intensities of NPE-to-PE (F ratios) under various experimental conditions are summarized in Figures 6 and 7. For normal PE-NPE cell couplets (norm, $N = 10$), there was a continuous LY dye diffusion from PE cell to NPE cell, as reflected by the progressive increase in F ratio, reaching a steady state ~10 minutes after rupture of the plasma membrane. Since the F ratio reached 1.70 ± 0.17 by 10 minutes and then remained stable until the end of the experiment, 10 minutes was chosen as the time point for the comparison of F ratios under various conditions. For couplets treated with nonselective gap junction inhibitor heptanol (3.5 mM, $N = 5$), the F ratio decreased with time and reached a steady value by 10 minutes (Fig. 6). At 10 minutes, the F ratio was found to be 0.16 ± 0.04 and remained at a low level. Compared with the control, heptanol inhibited the gap junction permeability by 90%. For couplets treated with scrambled siRNA (siScram, $N = 7$), the change in F ratio was similar to that of normal couplets, as demonstrated in Figure 6. The F ratio was found to be 1.79 ± 0.32 at 10 minutes. The F ratios showed no statistically significant difference between control and siScram-treated groups at all time points ($P > 0.05$, 1-way ANOVA), indicating that the scrambled siRNA did not affect the gap junction permeability of the cell couplets. For the cell couplets transfected with siRNA against Cx43 (siCx43, $N = 8$), the F ratio was found to decrease rapidly in the first 3 minutes and become stable by 5 minutes. At 10 minutes, the F value was
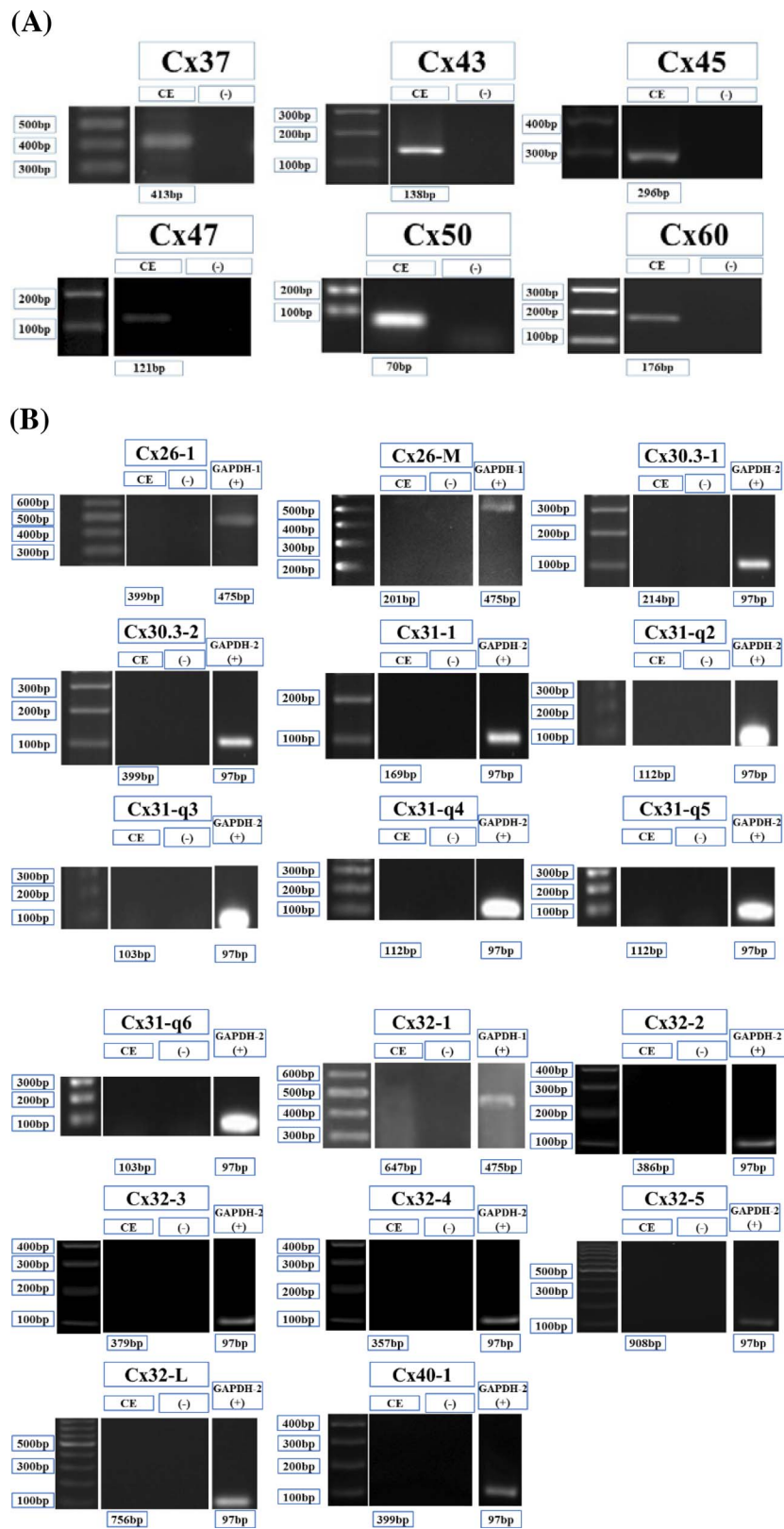
Figure 1. Expression of Cx isoforms in porcine CE detected by RT-PCR. (**A**) The presence of Cx37, Cx43, Cx45, Cx47, Cx50, and Cx60 mRNA expression in porcine CE. (**B**) Cx26, Cx30.3, Cx31, Cx32, and Cx40 mRNA expression were not detected in porcine CE. (−) no template negative control (NTC); GAPDH-1 or GAPDH-2 (+): control using GAPDH primers. At least three biologic replicates were performed for each pair of primers.
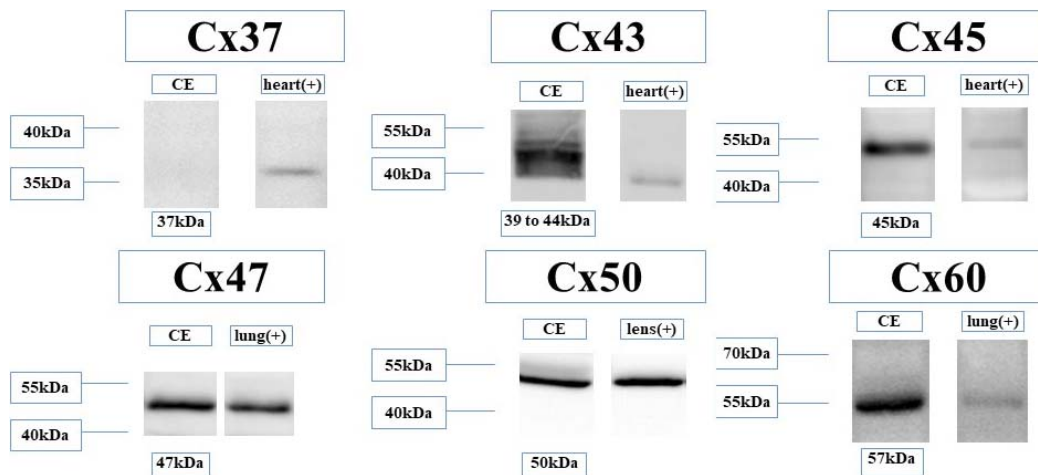
FIGURE 2. Expression of Cx isoforms in porcine CE detected by Western blot. Protein expression was detected for Cx43, Cx45, Cx47, Cx50, and Cx60, but not Cx37. At least three biologic replicates were performed for each Cx.

0.21 ± 0.05, corresponding to a 88% reduction in F ratio as compared to siScram (Fig. 7). No significant difference in F ratios was observed between the heptanol and siCx43 groups throughout the experimental period ($P > 0.05$, 1-way ANOVA). Our results suggested that the inhibitory effect of Cx43 knockdown on dye transfer rate was similar to that of the non-selective gap junction blocker heptanol.

DISCUSSION

In this study, we have characterized the gap junctions in porcine CE. Our results showed that Cx43 was the most abundant Cx present in porcine CE, located primarily on the apical surface linking between PE and NPE cells. Knockdown of Cx43 with siRNA caused a significant reduction of gene and protein expressions, resulting in a ~90% reduction of dye diffusion from PE to NPE cells. Our findings support the hypothesis that Cx43 provides a major conduit for fluid movement across porcine PE-NPE cell couplets.

Species Variation in Aqueous Humor Secretion

Normal IOP is maintained by the balance of the secretion and drainage of AH. Secretion of AH is driven by a transepithelial fluid secretion across the CE through the intercellular gap junctions between PE and NPE cells. It has been suggested that
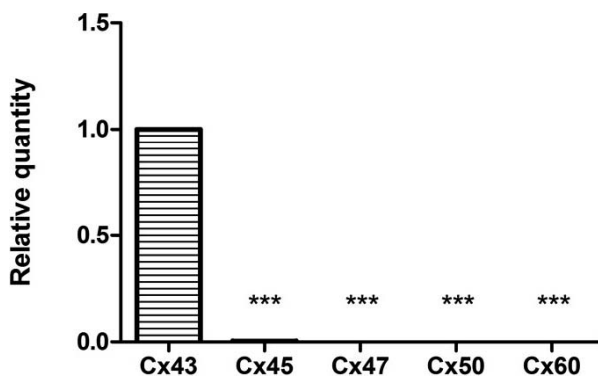

FIGURE 3. Relative quantity of Cx in native porcine CE by qPCR. The expression of Cx43 was found to be over 200-fold higher than those of all other expressed Cx ($N = 6$, ***$P < 0.001$, 1-way ANOVA, compared to Cx43).

the mechanism of AH secretion displays species variation.[25] For example, HCO_3^- secretion was shown to be important for driving AH secretion in rabbits.[26–29] However, no net HCO_3^- flux was detected across bovine CE.[30] Instead, Cl^- transport has been reported to play an important role in mediating AH formation in many experimental species including cat,[31] ox,[4] and pig.[5] These results indicate that the transport mechanisms and regulation of AH secretion may vary among species. Porcine eye may be a good animal model to mimic human ocular conditions because access to human eyes is limited while fresh porcine eyes are readily available; the physical dimensions and anatomic properties of porcine eyeball are similar to those of humans[20,21]; the electrolyte composition of the AH as well as the characteristics of AH dynamics in pig are similar to those in humans[1,19]; and the biocompatibility of pig and human eyes has been demonstrated in an artificial corneal graft study.[32] Our recent findings of cAMP- and forskolin-induced Isc stimulation in porcine CE[22] are also in good agreement with the results obtained for the human ciliary process,[23] suggesting that pig may be a good animal model for studying AH dynamics.

Characterization of Cx in the CE of Mammalian Eyes

Heptanol was previously shown to inhibit the transepithelial potential difference and fluid transfer across CE in various species,[3–6] indicating that the modulation of gap junction permeability may play a vital role in regulating AH inflow and thereby IOP. Several Cx isoforms have previously been identified in the CE of different species.[7,13–17] However, the relative contribution of these Cx in mediating the secretion of AH is not entirely clear. We have demonstrated the presence of Cx43, Cx45, Cx47, Cx50, and Cx60 in porcine CE, of which Cx43 is the most abundantly expressed (200-fold higher than all other Cx). As shown in Figure 2, the distribution of Cx43 protein in the CE is much wider than the control heart Cx43, possibly reflecting the post-translational modifications in the porcine preparation. In addition, Cx43 was found to be localized primarily at the apical borders connecting the PE and NPE layers. Our result is consistent with a recent study in which both Cx43 and Cx50 were detected in the porcine CE using an immunohistochemical approach.[18] On the other hand, Cx26, Cx31, and Cx40, that have been reported in rat[14,15] and bovine CE,[13] were not observed in porcine CE, supporting the possibility of species variation in the transport
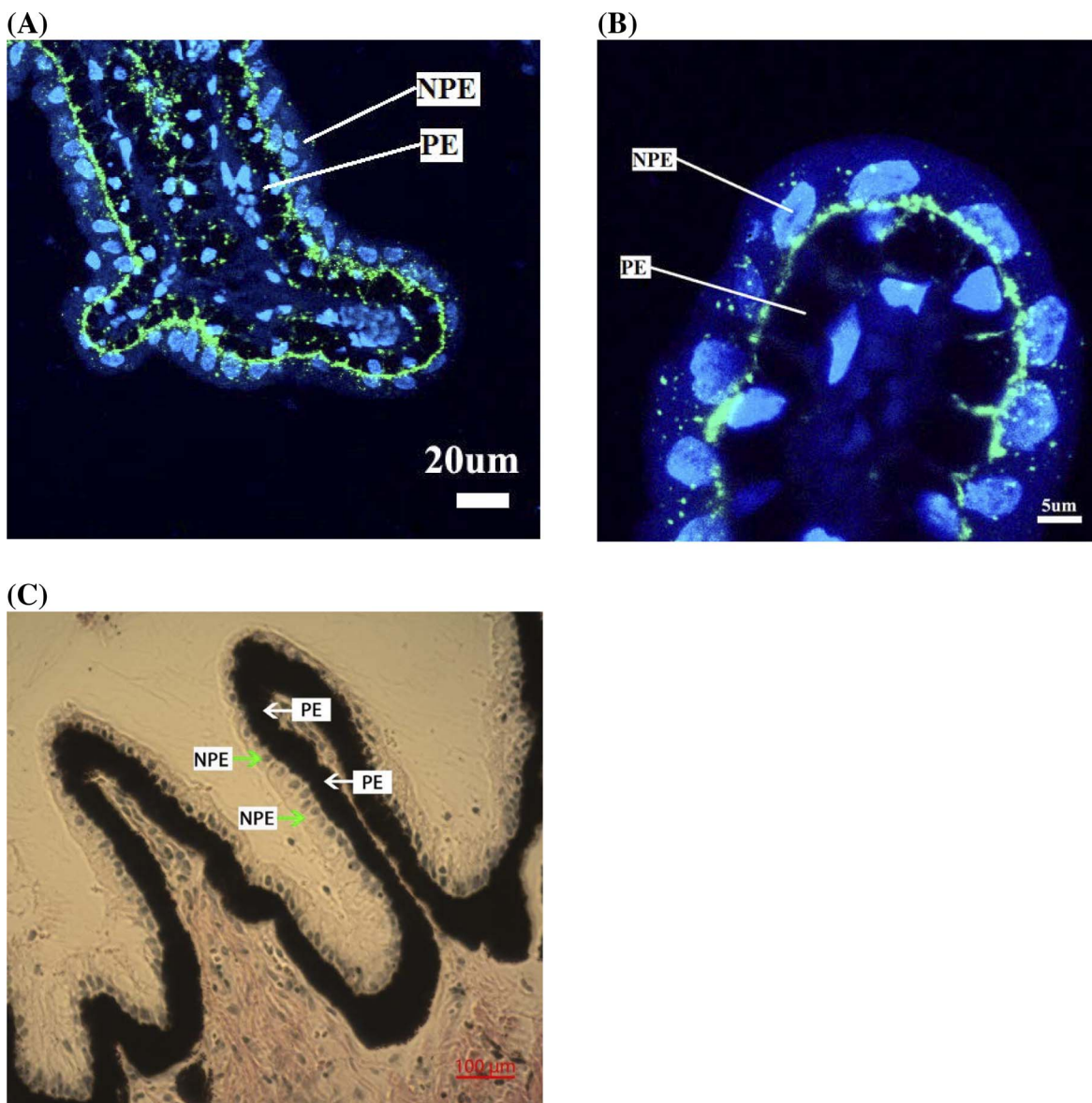
FIGURE 4. Immuno-localization of Cx43 in porcine CE under (**A**) low and (**B**) high magnification. Cx43 (*green*) was primarily detected at the apical membrane connecting PE and NPE layers and at the basolateral side of the PE layers. (**C**) Adjacent part of the same tissue treated with H&E stain.
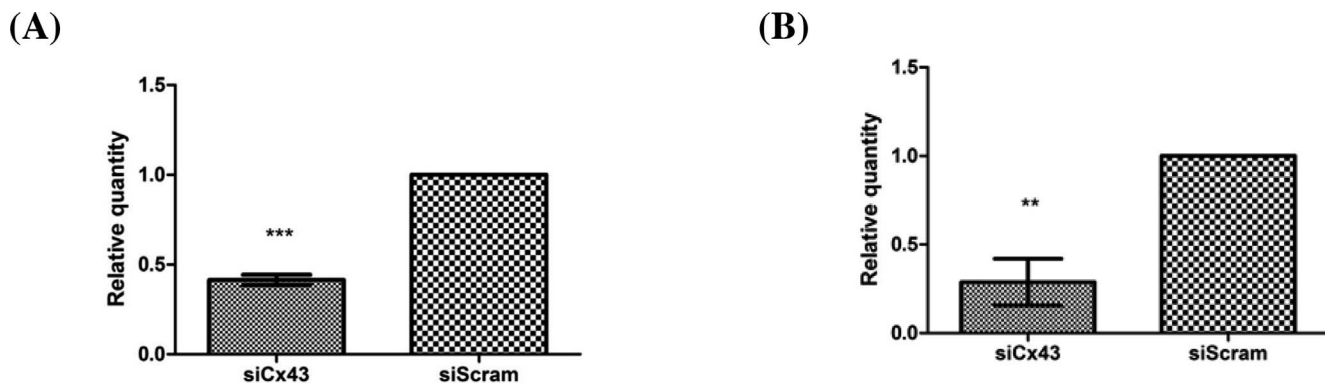

FIGURE 5. Relative quantity of Cx43 (**A**) mRNA ($N = 4$, ***$P < 0.001$) and (**B**) protein ($N = 3$, **$P < 0.01$) expressions in porcine CE after siRNA transfection for 24 hours. siCx43, porcine CE treated with siRNA against Cx43; siScram, porcine CE treated with scrambled siRNA.
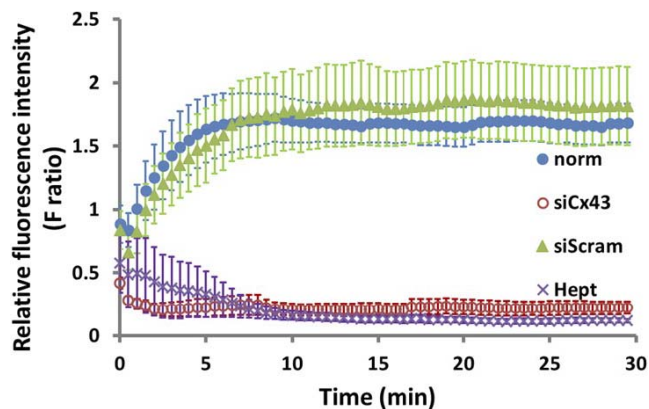
Investigative Ophthalmology & Visual Science

FIGURE 6. Relative fluorescence intensity (F ratio) over time under various conditions. norm, normal isolated porcine PE-NPE cell couplets ($N = 10$); siCx43, couplets treated with siRNA against Cx43 ($N = 8$); siScram, couplets treated with scrambled siRNA ($N = 7$); Hept, couplets treated with 3.5 mM heptanol, a non-selective gap junction blocker ($N = 5$).
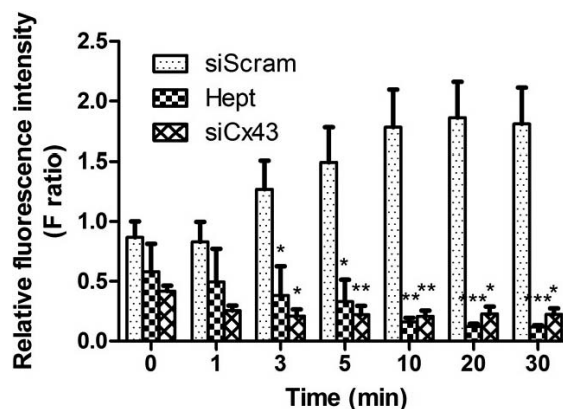

FIGURE 7. Relative fluorescence intensity (F ratio) at selected time points under various conditions (*$P < 0.05$, **$P < 0.01$, ***$P < 0.001$, 1-way ANOVA compared to siScram control condition).

mechanism. Although Cx37 was detected at mRNA level, its protein expression was not observed in our study. One possibility was that the quantity of Cx37 protein was not sufficient for detection by immunoblotting. The finding is in agreement with a recent study in which Cx37 was not detected in porcine CE.[18]

Role of Cx43 in Regulating Gap Junction Permeability

We speculate that Cx43 may provide an important route of solute transfer between the two layers because it is the most abundant Cx isoform expressed in porcine CE and is primarily located at the apical surface between PE and NPE cells. Therefore, we have evaluated the functional significance of Cx43 in mediating fluid movement across porcine PE-NPE cell couplets using LY dye transfer technique. It has been reported that Cx isoforms display selectivity for fluorescent probes and LY has been found to permeate most Cx isoforms including Cx43.[33] After 24-hour transfection with siRNA against Cx43, the gene and protein expressions of Cx43 in porcine CE cells was reduced by 60%–70%, thereby resulting in an inhibition of fluid flow by ∼90% in PE-NPE cell couplets, compared to control. It was noted that the scrambled siRNA did not affect the dye transfer when compared to the untreated control throughout the experiment (Fig. 6), suggesting that the scrambled siRNA may not alter the gap junctions' permeability. On the other hand, the inhibition exerted by Cx43 siRNA knockdown was similar to that of heptanol, indicating that Cx43 may constitute the major gap junction channel between PE and NPE cells facilitating fluid movement across porcine preparation.[6] It is observed that the relative contribution of Cx43 in mediating AH secretion in pigs is possibly higher than in cows, as the fluid transfer was only inhibited by ∼60% in bovine CE.[7]

Cx43 as a Target for Glaucoma Treatment

Currently, there is no clinically-available anti-glaucoma drug that lowers IOP by uncoupling the intercellular gap junctions between PE and NPE cells. Therefore, understanding the specific Cx isoforms in the CE is important as it may shed light on the development of a novel ocular hypotensive agent. Inactivation of Cx43 in mouse CE leads to a reduction of IOP,[17] further supporting its potential significance in glaucoma

treatment. It has been shown that Cx43 is present in the neighboring tissues including the cornea[34] and crystalline lens.[35] No adverse complications in the cornea and surrounding tissues resulted from down-regulation of Cx43 in rats.[36] In contrast, inhibition of Cx43 was reported to aid corneal wound healing in humans both in vitro[37] and in vivo.[38] Cataract formation did not occur in the crystalline lens of Cx43 knockout mice.[39] In the retina, gap junctions have been shown to be involved in spreading apoptotic signals in the retinal ganglion cells.[40] Meclofenamic acid, a non-selective gap junction blocker, has been demonstrated to reduce retinal ganglion cell loss by 70%.[40] Blockade of Cx43 has also been suggested to enhance neuronal cell survival,[41] indicating the potential role of Cx43 in glaucoma therapy. Currently, none of the existing antiglaucoma agents targets Cx43. Together with the reduction in fluid flow across bovine PE-NPE cell couplets after Cx43 siRNA treatment[7] and reduced IOP in mouse with inactivated Cx43 in NPE cells,[17] our findings support the functional significance of Cx43 as a potential target for glaucoma management.

References

1. Civan MM. Formation of the aqueous humor: transport components and their integration. In: Civan MM, ed. *The Eye's Aqueous Humor*. San Diego: Elsevier Inc.; 2008:2–45.

2. Shahidullah M, Al-Malki WH, Delamere NA. Mechanism of Aqueous humor secretion, its regulation and relevance to glaucoma. In: Rumelt S, ed. *Glaucoma - Basic and Clinical Concepts*. London: IntechOpen; 2011:3–32.

3. Wolosin JM, Candia OA, Peterson-Yantorno K, Civan MM, Shi XP. Effect of heptanol on the short circuit currents of cornea and ciliary body demonstrates rate limiting role of heterocellular gap junctions in active ciliary body transport. *Exp Eye Res*. 1997;64:945–952.

4. Do CW, To CH. Chloride secretion by bovine ciliary epithelium: a model of aqueous humor formation. *Invest Ophthalmol Vis Sci*. 2000;41:1853–1860.

5. Kong CW, Li KK, To CH. Chloride secretion by porcine ciliary epithelium: new insight into species similarities and differences in aqueous humor formation. *Invest Ophthalmol Vis Sci*. 2006;47:5428–5436.

6. Law CS, Candia OA, To CH. Inhibitions of chloride transport and gap junction reduce fluid flow across the whole porcine ciliary epithelium. *Invest Ophthalmol Vis Sci*. 2009;50:1299–1306.

7. Wang Z, Do CW, Valiunas V, et al. Regulation of gap junction coupling in bovine ciliary epithelium. *Am J Physiol Cell Physiol*. 2010;298:C798–C806.

8. Sosinsky G. Gap junction structure: new structures and new insights. In: Peracchia C, ed. *Gap Junctions: Molecular Basis of Cell Communication in Health and Disease*. San Diego, CA: Academic Press; 2000.

9. Beyer EC, Berthoud VM. The family of connexin genes. In: AL, Harris Locke D, eds. *Connexins*. New York, NY: Humana Press; 2009:3–26.

10. Hussain MU. *Connexins: The Gap Junction Proteins*. New Delhi: Springer; 2014.

11. Raviola G, Raviola E. Intercellular junctions in the ciliary epithelium. *Invest Ophthalmol Vis Sci*. 1978;17:958–981.

12. Raviola G. The fine structure of the ciliary zonule and ciliary epithelium. With special regard to the organization and insertion of the zonular fibrils. *Invest Ophthalmol Vis Sci*. 1971;10:851–869.

13. Coca-Prados M, Ghosh S, Gilula NB, Kumar NM. Expression and cellular distribution of the alpha 1 gap junction gene product in the ocular pigmented ciliary epithelium. *Curr Eye Res*. 1992;11:113–122.

14. Wolosin JM, Schütte M, Chen S. Connexin distribution in the rabbit and rat ciliary body. A case for heterotypic epithelial gap junctions. *Invest Ophthalmol Vis Sci*. 1997;38:341–348.

15. Coffey KL, Krushinsky A, Green CR, Donaldson PJ. Molecular profiling and cellular localization of connexin isoforms in the rat ciliary epithelium. *Exp Eye Res*. 2002;75:9–21.

16. Calera MR, Topley HL, Liao Y, Duling BR, Paul DL, Goodenough DA. Connexin43 is required for production of the aqueous humor in the murine eye. *J Cell Sci*. 2006;119:4510–4519.

17. Calera MR, Wang Z, Sanchez-Olea R, Paul DL, Civan MM, Goodenough DA. Depression of intraocular pressure following inactivation of connexin43 in the nonpigmented epithelium of the ciliary body. *Invest Ophthalmol Vis Sci*. 2009;50:2185–2193.

18. Shahidullah M, Delamere NA. Connexins form functional hemichannels in porcine ciliary epithelium. *Exp Eye Res*. 2014;118:20–29.

19. Shahidullah M, Yap M, To CH. Cyclic GMP, sodium nitroprusside and sodium azide reduce aqueous humour formation in the isolated arterially perfused pig eye. *Br J Pharmacol*. 2005;145:84–92.

20. Beauchemin ML. The fine structure of the pig's retina. *Albrecht Von Graefes Arch Klin Exp Ophthalmol*. 1974;190:27–45.

21. Simoens P, De Schaepdrijver L, Lauwers H. Morphologic and clinical study of the retinal circulation in the miniature pig. A: morphology of the retinal microvasculature. *Exp Eye Res*. 1992;54:965–973.

22. Cheng AK, Civan MM, To CH, Do CW. cAMP stimulates transepithelial short-circuit current and fluid transport across porcine ciliary epithelium. *Invest Ophthalmol Vis Sci*. 2016;57:6784–6794.

23. Wu RY, Ma N, Hu QQ. Effect of cAMP on short-circuit current in isolated human ciliary body. *Chin Med J (Engl)*. 2013;126:2694–2698.

24. Livak KJ, Schmittgen TD. Analysis of relative gene expression data using real-time quantitative PCR and the 2(-Delta Delta C(T)) Method. *Methods*. 2001;25:402–408.

25. Do CW, Civan MM. Species variation in biology and physiology of the ciliary epithelium: similarities and differences. *Exp Eye Res*. 2009;88:631–640.

26. Wolosin JM, Chen M, Gordon RE, Stegman Z, Butler GA. Separation of the rabbit ciliary body epithelial layers in viable form: identification of differences in bicarbonate transport. *Exp Eye Res*. 1993;56:401–409.

27. Crook RB, Takahashi K, Mead A, Dunn JJ, Sears ML. The role of NaKCl cotransport in blood-to-aqueous chloride fluxes across rabbit ciliary epithelium. *Invest Ophthalmol Vis Sci*. 2000;41:2574–2583.

28. Candia OA, To CH, Gerometta RM, Zamudio AC. Spontaneous fluid transport across isolated rabbit and bovine ciliary body preparations. *Invest Ophthalmol Vis Sci*. 2005;46:939–947.

29. Gerometta RM, Malgor LA, Vilalta E, Leiva J, Candia OA. Cl-concentrations of bovine, porcine and ovine aqueous humor are higher than in plasma. *Exp Eye Res*. 2005;80:307–312.

30. To CH, Do CW, Zamudio AC, Candia OA. Model of ionic transport for bovine ciliary epithelium: effects of acetazolamide and HCO. *Am J Physiol Cell Physiol*. 2001;280:C1521–C1530.

31. Holland MG, Gipson CC. Chloride ion transport in the isolated ciliary body. *Invest Ophthalmol Vis Sci*. 1970;9:20–29.

32. Yoshida J, Oshikata-Miyazaki A, Yokoo S, Yamagami S, Takezawa T, Amano S. Development and evaluation of porcine atelocollagen vitrigel membrane with a spherical curve and transplantable artificial corneal endothelial grafts. *Invest Ophthalmol Vis Sci*. 2014;55:4975–4981.

33. Kanaporis G, Brink PR, Valiunas V. Gap junction permeability: selectivity for anionic and cationic probes. *Am J Physiol Cell Physiol*. 2011;300:C600–C609.

34. Zhai J, Wang Q, Tao L. Connexin expression patterns in diseased human corneas. *Exp Ther Med*. 2014;7:791–798.

35. Shakespeare TI, Mathias RT, White TW. Connexins in lens development and disease. In: Harris A, Locke D, eds. *Connexins: A Guide*. New York: Springer; 2009.

36. Moore K, Ghatnekar G, Gourdie RG, Potts JD. Impact of the controlled release of a connexin 43 peptide on corneal wound closure in an STZ model of type I diabetes. *PLoS One*. 2014;9:e86570.

37. Elbadawy HM, Mirabelli P, Xeroudaki M, et al. Effect of Connexin 43 inhibition by the mimetic peptide Gap27 on corneal wound healing, inflammation and neovascularization. *Br J Pharmacol*. 2016;173:2880–2893.

38. Ormonde S, Chou CY, Goold L, et al. Regulation of connexin43 gap junction protein triggers vascular recovery and healing in human ocular persistent epithelial defect wounds. *J Membr Biol*. 2012;245:381–388.

39. DeRosa AM, Mese G, Li L, et al. The cataract causing Cx50-S50P mutant inhibits Cx43 and intercellular communication in the lens epithelium. *Exp Cell Res*. 2009;315:1063–1075.

40. Akopian A, Atlasz T, Pan F, et al. Gap junction-mediated death of retinal neurons is connexin and insult specific: a potential target for neuroprotection. *J Neurosci*. 2014;34:10582–10591.

41. Chew SS, Johnson CS, Green CR, Danesh-Meyer HV. Role of connexin43 in central nervous system injury. *Exp Neurol*. 2010;225:250–261.